Current Topics in Biophysics 2005, 29(1-2), 89-93

RECENT DEVELOPMENTS IN TIME DOMAIN SPECTROSCOPIC EPR IMAGING

COLIN MAILER, SUNDRAMOORTHY V. SUBRAMANIAN, CHARLES A. PELIZZARI, HOWARD J. HALPERN

Center for EPR Imaging In Vivo Physiology, Department of Radiation and Cellular Oncology, University of Chicago, Chicago IL

Our recent developments in time domain spin echo EPR spectral-spatial imaging will be presented. In particular the usefulness of spin echoes in obtaining spectroscopic EPR images will be presented.

INTRODUCTION

The aim of this presentation is to describe recent developments in our laboratory in spectroscopic imaging (or spectral-spatial imaging) using time domain techniques. The scientific goal of this work is to obtain images of physiological parameters, such as oxygen concentration, in animals (Elas, Williams, Parasca, Mailer, Pelizzari, Lewis, River, Karczmar, Barth, & Halpern, 2003; Halpern, Yu, Peric, Barth, Grdina & Teicher, 1994; Williams, al Hallaq, Chandramouli, Barth, Rivers, Lewis, Galtsev, Karczmar & Halpern, 2002). Knowledge of the distribution of the oxygen concentration in tumors is a particularly important for radiation therapy and chemotherapy, as well as newer techniques involving anti-angiogenesis drugs.

Most of the work in our laboratory has been done with conventional continuous wave electron paramagnetic resonance (CW-EPR) at ~250 MHz radio frequency (Halpern, Spencer, Vanpolen, Bowman, Nelson, Dowey & Teicher, 1989; Rinard, Quine, Eaton, Eaton, Barth, Pelizzari & Halpern, 2002b). There are some particular requirements for animal imaging – fast scan ability, rapid phase and frequency correction for animal movement, easy access to the animal etc. that differentiate our instrument from higher frequency ones – but pose no fundamental challenges. Images are reconstructed from projections consisting of field swept spectra in the presence of field gradients. A collection of spectra obtained using a set of gradients in different directions allows one to use filtered back projection (FBP) to reconstruct a spatial image of the object. In order to obtain a spectroscopic image extra data collection is carried out – sets of spectra are obtained with the amplitudes of the gradient in a particular direction being stepped from a positive maximum to a negative maximum. Such a spectroscopic image has a spectrum in each spatial voxel (Hyslop, Woods & Lauterbur, 1995; Matsumoto, Chandrika, Lohman, Mitchell, Krishna & Subramanian, 2003). Oxygen causes broadening of these voxel spectra proportional to the oxygen concentration and hence oxygen images can be obtained (Elas *et al.*, 2003; Mailer, Robinson, Williams & Halpern, 2003).

There are some disadvantages to CW-EPR imaging – such as animal motion induced baseline artifacts – but the major problem is loss of signal due to gradient broadening. This arises because the Zeeman field modulation/ phase sensitive detector technique used produces signals whose height is inversely proportional to the square of the line width – this means that high amplitude gradients which broaden the natural EPR line widths by approximately an order of magnitude reduce the signal by one to two orders of magnitude. Spectroscopic image acquisition time is increased by about a factor of two more than for a simple spatial image.

Time domain spectroscopic imaging can offer some advantages over CW imaging – the DC field does not have to be swept, no modulation is required and hence the signal only decreases proportional to the gradient strength and not the square of it, animal motion problems are reduced. This technique is not without disadvantages – the microsecond relaxation times of EPR spin probes mean that data collection is on the nanosecond to microsecond time scale (Yong, Harbridge, Quine, Rinard, Eaton, Eaton, Mailer, Barth & Halpern, 2001), that high RF powers are required (hundreds of Watts) and that rapid signal averaging is needed

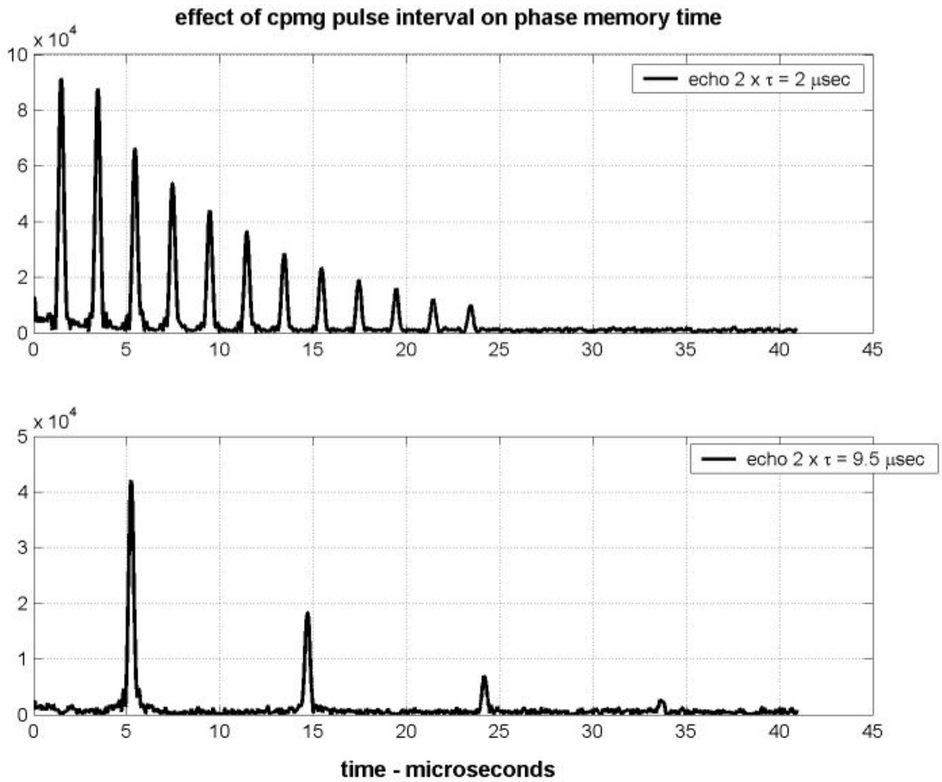

Fig. 1. Plot of echoes obtained with two different CPMG pulse spacings. Top: $\tau = 1$ μs 12 echoes. Bottom: $\tau = 4.75$ μs 3 echoes. Echo decay rate = 0.1 Mradian/sec (T_{2e} = 10 μsec).

(Subramanian, Murugesan, Devasahayam, Cook, Afeworki, Pohida, Tschudin, Mitchell & Krishna, 1999). As a result time domain spectroscopic imaging is confined to a few laboratories in the world.

There are three main ways to perform imaging in the time domain EPR (TD-EPR):

1. Free induction decay (FID) detection. The signal is the time decay response of the sample to a short pulse of RF power. Fourier Transform (FT) of the decay gives the unmodulated CW-EPR spectrum and a set of such spectra for different gradient amplitudes and directions after FBP reconstruction will produce a similar spectroscopic image.(Subramanian *et al.*, 1999)
2. Single point imaging (SPI) detection. The SPI detection is described elsewhere in these Proceedings and is capable of very fast imaging (Subramanian, Devasahayam, Murugesan, Yamada, Cook, Taube, Mitchell, Lohman & Krishna, 2002).
3. Echo detection. There are a number of advantages to using spin echoes obtain with a series of RF pulses: The echoes can be made to occur well after the instrumental dead time reducing dead time artifacts and multiple echoes can be collected in one experiment and their decay gives spectral information as will be described below.

EXPERIMENTAL

The pulse spectrometer is controlled by a Bruker Elexys system console containing a Specjet digitizer/averager and a Patternjet pulse programmer. The RF bridge is home-built and largely follows standard published designs. (Rinard *et al.*, 2002b) A unique feature, however, is the use of a bimodal crossed-loop resonator (CLR) for stimulation and detection (Rinard, Quine, Eaton & Eaton, 2002a; Rinard, Quine, Ghim, Eaton & Eaton, 1996). It consists of two orthogonally intersecting re-entrant resonators whose RF isolation can be adjusted to be better than 50 dB even when both resonate at the same frequency. This gives our system a very short dead time of ~ 250 nanoseconds as very little of the high power input pulse leaks through into the detection system. The Carr-Purcell-Meiboom-Gill (CPMG) pulse sequence is used to form the echoes because it cancels pulse imperfections:

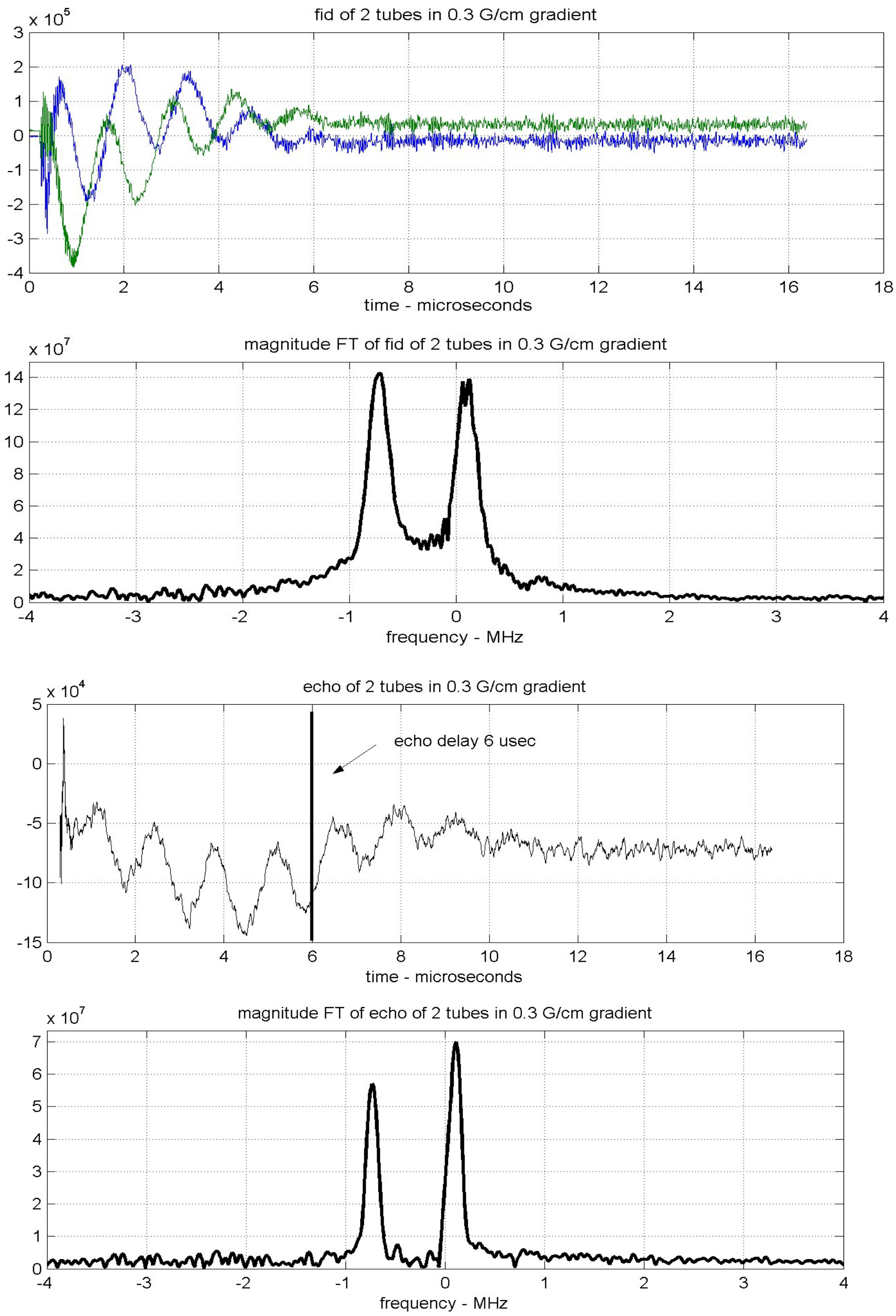

Fig. 2. FID and echo compared for two 0.3 mm diameter tubes separated by 18 mm.

$$(\pi/2)_x - \tau - (\pi)_y - 2\tau - (\pi)_y - 2\tau - (\pi)_y \ldots$$

The samples used were either a cylindrical phantom 1.5 cm diameter or two 3 mm diameter tubes containing ~0.4 mM of deoxygenated deuterated trityl compound supplied by Nycomed (now GE).(Ardenjaer-Larsen, Laursen, Leunbach, Ehnholm, Wistrand, Petersson & Golman, 1998). This trityl was chosen because it has very long T_{2e} and T_{1e} and very little inhomogeneous broadening resulting in an extremely narrow line width of ~2.5 µTesla (25 milligauss).

Figure 1 shows the echoes obtained from the cylindrical phantom with two different pulse spacings. Fitting the decay of the echoes gave the same time constant, showing that under the 10 mTesla/meter (1 gauss/cm) gradients used no spectral diffusion processes contribute to the decays. If they did then the calibration of the system would depend on the pulse sequence used which would complicate interpretation of the results (Harbridge,

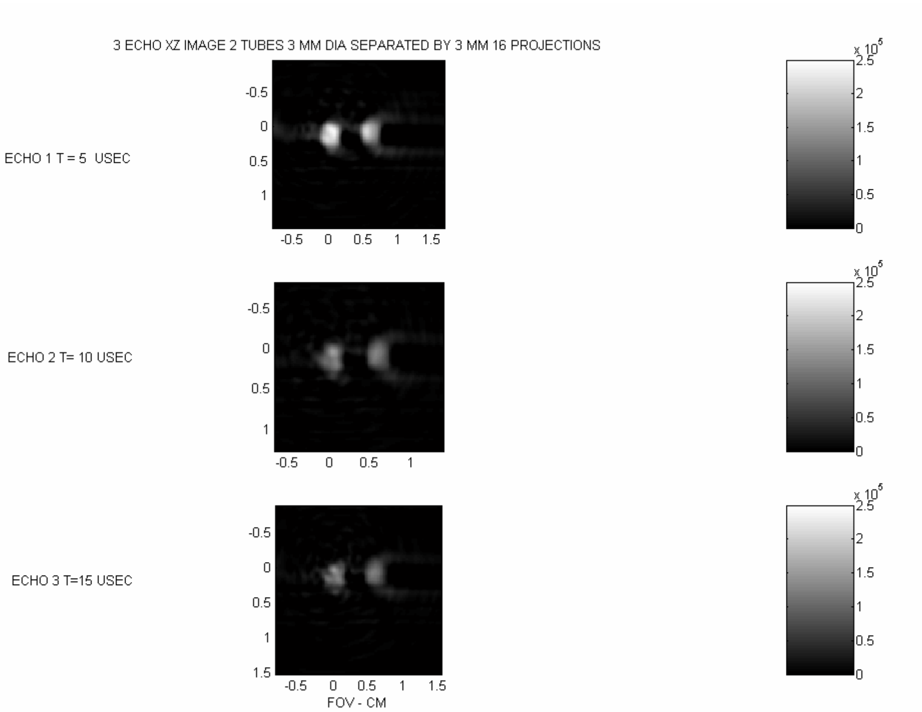

Fig. 3. Two dimensional cross section images from three-echo set of 16 projections. The intensity scale on all im-

Eaton & Eaton, 1998). Figure 2 shows the superior performance of the echo relative to the FID for obtaining an accurate Fourier Transform. Because the echo is obtained long after the dead time the detection system can operate optimally. The record length of the echo trace is also much longer. The FT of the echo decay gives a much narrower projection of the signal from the two tubes, and the separation (in frequency units) exactly agrees with the gradient strength and physical separation of the tubes. The FID projection is clearly broader and does not represent the physical separation of the tubes nearly as well. Two dimensional mages reconstructed from a three-echo set of 16 projections of the two tubes are shown in Figure 3.

DISCUSSION

These results show that the use of spin echoes gives excellent spatial images but also the decay of the signal in successive echoes shows one measure the decay time of the probe in any individual voxel. A spatial map of decay times is exactly what we need to measure the oxygen concentration in the object. The deoxygenated trityl relaxation rate of ~0.1 Mradian/sec (T_{2e} ~ 10 μsec) and the small relaxivity of oxygen ~0.085 Mradian/sec/torr (0.48 milligauss/torr) means that the observed decay rate is very sensitive to low levels of oxygen. The time range is also excellent for obtaining images from the echoes. We believe that decay rates as short as 1 Mradian/sec - equivalent to 100 torr of oxygen - can be imaged with the echo technique so our dynamic range is large. Simple calculation shows that an echo image obtained at ~25 μsec would have no more than 5% of the voxels with oxygen levels greater than 10 torr so we have the possibility of high contrast as well. Although much remains to be done it is clear that echo imaging has great potential to perform spectroscopic imaging in a very effective way.

REFERENCES

Ardenjaer-Larsen J. H., Laursen I., Leunbach I., Ehnholm G., Wistrand L.-G., Petersson J. S., & Golman K. (1998). EPR and DNP properties of certain novel single electron contrast agents intended for oximetric imaging. *J. Magn. Reson.,* **133**, 1-12.

Elas M., Williams B. B., Parasca A., Mailer C., Pelizzari C. A., Lewis M. A., River J. N., Karczmar G. S., Barth E. D., & Halpern H. J. (2003). Quantitative tumor oxymetric images from 4D electron paramagnetic resonance imaging (EPRI): Methodology and comparison with blood oxygen level-dependent (BOLD) MRI. *Magnetic Resonance in Medicine,* **49**, 682-691.

Halpern H. J., Spencer D. P., Vanpolen J., Bowman M. K., Nelson A. C., Dowey E. M., & Teicher B. A. (1989). Imaging radio-frequency electron-spin-resonance spectrometer with high-resolution and Sensitivity for in vivo measurements. *Review of Scientific Instruments,* **60**, 1040-1050.

Halpern H. J., Yu C., Peric M., Barth E., Grdina D. J. & Teicher B. A. (1994). Oxymetry deep in tissues with low-frequency electron-paramagnetic-resonance. *Proceedings of the National Academy of Sciences of the United States of America,* **91**, 13047-13051.

Harbridge J. R., Eaton G. R. & Eaton S. S. (1998). Impact of spectral diffusion on apparent relaxation times for the stable radical in irradiated glycylglycine. *Modern Applications of EPR/ESR: From Biophysics to Materials Science, Proceedings of the Asia-Pacific EPR/ESR Symposium, 1st, Kowloon, Hong Kong, Jan. 20-24, 1997*, pp. 220-225.

Hyslop W. B., Woods R. K. & Lauterbur P. C. (1995). 4-Dimensional Spectral-Spatial Imaging Using Projection Reconstruction. *IEEE Transactions on Medical Imaging,* **14**, 374-383.

Mailer C., Robinson B. H., Williams B. B. & Halpern H. J. (2003). Spectral fitting: The extraction of crucial information from a spectrum and a spectral image. *Magnetic Resonance in Medicine,* **49**, 1175-1180.

Matsumoto K., Chandrika B., Lohman J. A. B., Mitchell J. B., Krishna M. C. & Subramanian S. (2003). Application of continuous-wave EPR spectral-spatial image reconstruction techniques for in vivo oxymetry: Comparison of projection reconstruction and constant-time modalities. *Magnetic Resonance in Medicine,* **50**, 865-874.

Rinard G. A., Quine R. W., Eaton G. R. & Eaton S. S. (2002a). 250 MHz crossed loop resonator for pulsed electron paramagnetic resonance. *Magn. Reson. Engineer.,* **15**, 37-46.

Rinard G. A., Quine R. W., Eaton G. R., Eaton S. S., Barth E. D., Pelizzari C. A. & Halpern, H. J. (2002b). Magnet and gradient coil system for low-field EPR imaging. *Concepts in Magnetic Resonance,* **15**, 51-58.

Rinard G. A., Quine R. W., Ghim B. T., Eaton S. S. & Eaton G. R. (1996). Easily tunable crossed-loop (bimodal) EPR resonator. *Journal of Magnetic Resonance, Series A,* **122**, 50-57.

Subramanian S., Devasahayam N., Murugesan R., Yamada K., Cook J., Taube A., Mitchell J. B., Lohman, J. A. B. & Krishna M. C. (2002). Single-point (constant-time) imaging in radiofrequency Fourier transform electron paramagnetic resonance. *Magnetic Resonance in Medicine,* **48**, 370-379.

Subramanian S., Murugesan R., Devasahayam N., Cook J. A., Afeworki M., Pohida T., Tschudin R. G., Mitchell J. B. & Krishna M. C. (1999). High-speed data acquisition system and receiver configurations for time-domain radiofrequency electron paramagnetic resonance spectroscopy and imaging. *Journal of Magnetic Resonance,* **137**, 379-388.

Williams B. B., al Hallaq H., Chandramouli G. V. R., Barth E. D., Rivers J. N., Lewis M., Galtsev V. E., Karczmar G. S. & Halpern, H. J. (2002). Imaging spin probe distribution in the tumor of a living mouse with 250 MHz EPR: Correlation with BOLD MRI. *Magnetic Resonance in Medicine,* **47**, 634-638.

Yong L., Harbridge J., Quine R. W., Rinard G. A., Eaton S. S., Eaton G. R., Mailer C., Barth E. & Halpern, H. J. (2001). Electron spin relaxation of triarylmethyl radicals in fluid solution. *Journal of Magnetic Resonance,* **152**, 156-161.